

DC-AR: Efficient Masked Autoregressive Image Generation with Deep Compression Hybrid Tokenizer

Yecheng Wu Junyu Chen Zhuoyang Zhang Enze Xie Jincheng Yu
Junsong Chen Jinyi Hu Yao Lu Song Han Han Cai
NVIDIA

<https://github.com/dc-ai-projects/DC-AR>



Figure 1. **DC-AR** is a cutting-edge masked autoregressive text-to-image generation framework. In comparison to other leading masked autoregressive models and diffusion models, DC-AR delivers **1.5-7.9 \times** higher throughput and **2.0-3.5 \times** lower latency, all while achieving state-of-the-art quality on text-to-image generation benchmarks.

Abstract

We introduce **DC-AR**, a novel masked autoregressive (AR) text-to-image generation framework that delivers superior image generation quality with exceptional computational efficiency. Due to the tokenizers’ limitations, prior masked AR models have lagged behind diffusion models in terms of quality or efficiency. We overcome this limitation by introducing **DC-HT** — a deep compression hybrid tokenizer for AR models that achieves a $32\times$ spatial compression ratio while maintaining high reconstruction fidelity and cross-resolution generalization ability. Building upon **DC-HT**, we extend **MaskGIT** and create a new hybrid masked autore-

gressive image generation framework that first produces the structural elements through discrete tokens and then applies refinements via residual tokens. **DC-AR** achieves state-of-the-art results with a **gFID** of **5.49** on **MJHQ-30K** and an overall score of **0.69** on **GenEval**, while offering **1.5-7.9 \times** higher throughput and **2.0-3.5 \times** lower latency compared to prior leading diffusion and autoregressive models.

1. Introduction

The remarkable success of large language models (LLMs) has significantly propelled advancements in artificial intelligence. Central to this success are autoregressive models,

Correspondence to: Han Cai (hcail@nvidia.com).

which have gained widespread recognition due to their exceptional generalizability and robust scaling properties. Although primarily employed for natural language processing (NLP) tasks, autoregressive models have also been effectively adapted to image generation, leading to notable progress in the field [25, 28, 53, 60].

In contrast to diffusion models [4, 24, 38, 45, 65] which have dominated the current era, autoregressive models have recently garnered significant attention in image synthesis due to their unique advantages, such as enhanced connections with vision-language models [30, 43, 55, 63, 64, 67]. Typically, these approaches employ a visual tokenizer to transform images from pixel space into discrete tokens via vector quantization. Then, the models can process these visual tokens analogously to text tokens.

Previous research has explored various paradigms for autoregressive image generation, with masked autoregressive models emerging as an auspicious approach. Inspired by BERT [20] from the field of NLP, these models generate image token sequences through a progressive unmasking process. Unlike the popular GPT-like sequential next-token prediction paradigm, masked autoregressive models allow multiple tokens to be generated simultaneously at each step, significantly reducing the number of sampling steps and improving generation efficiency. Additionally, the masking and unmasking mechanism inherent to these models makes them naturally well-suited for image editing tasks. Since their introduction in MaskGIT [7], extensive research has been conducted to extend this method, leading to notable advancements and successes [2, 8, 15, 32, 34, 59, 62, 67, 69, 70].

However, compared to diffusion models, which utilize continuous tokens to represent images, autoregressive models face significant challenges for achieving competent efficiency and quality from the image tokenization process. The current standard practice for image tokenization employs an autoencoder with spatial reduction ratios of $8\times$ or $16\times$, where an image of size 256×256 is converted into 32×32 or 16×16 token, respectively. However, further reducing token numbers for improved efficiency remains critical, especially considering that computational costs increase when generating high-resolution images.

While DC-AE [11] has successfully achieved a high spatial compression ratio (e.g., $32\times$) for continuous tokenizers, it remains challenging to build a high-compression tokenizer that we can use for masked autoregressive models. In our experiments, we find directly applying DC-AE to the discrete tokenizer leads to awful reconstruction quality (Table 4). In parallel, some recent works [31, 71] adopt an alternative method to reduce tokens for discrete tokenizers by employing transformers to convert images into compact 1D latent sequences. Despite their impressive results, such designs break the spatial correspondence between 2D im-

age patches and tokens, making them unable to generalize across different resolutions. They cannot reuse weights of models trained on lower resolutions, making their training cost-prohibitive for high-resolution image synthesis.

This work introduces DC-AR, an efficient masked autoregressive framework for text-to-image generation. DC-AR incorporates DC-HT, a single-scale 2D tokenizer that achieves a spatial reduction ratio of $32\times$ while maintaining competitive reconstruction quality through hybrid tokenization. Hybrid tokenization, initially proposed by HART [53], is a technique designed to bridge the performance gap between discrete and continuous tokenizers. However, unlike HART, which employs a multi-scale tokenizer with a reduction ratio of $16\times$, training a single-scale tokenizer with a $32\times$ reduction ratio using conventional methods often results in suboptimal reconstruction quality.

To overcome these limitations, we propose a three-stage adaptation strategy (Figure 3) to train our tokenizer effectively. This strategy enables DC-HT to achieve performance comparable to 1D compact tokenizers at the same compression level while capable of generalizing across resolutions. Building on this tokenizer, we develop our text-to-image framework, which utilizes a hybrid coarse-to-fine generation process based on MaskGIT. We train our models with cross-entropy loss for discrete tokens and diffusion loss for residual tokens. At inference time, our framework first generates all discrete tokens through the unmasking process with a transformer model and then produces residual tokens via the denoising schedule of a lightweight diffusion head. These tokens are combined and de-tokenized to create the final output images, guided by the provided textual inputs.

We demonstrate the effectiveness of DC-AR across a diverse set of benchmarks. Our tokenizer achieves an rFID of **1.60** on ImageNet 256×256 [19], a performance comparable to 1D tokenizers with the same compression ratio. For text-to-image tasks, DC-AR achieves state-of-the-art results, with a gFID of **5.49** on MJHQ-30K and an overall score of **0.69** on GenEval. Additionally, DC-AR delivers **1.5-7.9** \times higher throughput and **2.0-3.5** \times lower latency compared to leading diffusion and masked autoregressive models, showcasing its great advantage as an efficient text-to-image generation framework. We summarize our contributions as follows:

- We build DC-HT that significantly reduces the token number to boost AR models’ efficiency while maintaining competitive reconstruction quality and cross-resolution generalization capacity.
- We introduce an effective three-stage adaptation strategy to improve DC-HT’s reconstruction quality.
- We build DC-AR based on DC-HT. DC-AR delivers a significant efficiency boost over prior masked AR models and diffusion models while providing better image generation quality.



Figure 2. Qualitative Comparison of Text-to-Image Generation Results Between DC-AR and Other Generative Models.

2. Related Work

Image Tokenizer. Since directly learning representation and generation in pixel space is computationally expensive and challenging, modern methods employ image tokenization to convert images into a latent space. These approaches primarily fall into two categories: strategies based on continuous latent token, pioneered by latent diffusion models [50] for diffusion models [3, 6, 44, 46], and methods based on discrete token [23, 58] for autoregressive models [7, 23].

Traditional tokenizers use $8\times$ or $16\times$ spatial compression ratios. Recent research suggests that images can be effectively represented with fewer tokens, leading to significant efficiency gains in the generation process [11, 65, 71]. DC-AE [11], featuring $32\times$ and higher compression ratios for continuous latents, follows the conventional 2D spatial tokenizer design. TiTok [71] established a new tokenization paradigm by employing transformer-based models to generate compact 1D global image representations with as few as 32 tokens, inspiring numerous subsequent works [1, 9, 10, 31, 73]. However, while practical at fixed resolutions, such compact 1D representations struggle to generalize across different resolutions—an essential advantage of traditional 2D spatial tokenizers. In this work, we adopt the established 2D spatial tokenization approach and develop a hybrid tokenizer with a $32\times$ compression ratio for efficient

autoregressive visual generation.

Autoregressive Image Generation. While diffusion models currently dominate text-to-image generation [12–14, 24, 33, 38, 41, 54, 56, 65, 66], autoregressive approaches have also demonstrated significant potentials [16, 25, 28, 60]. Autoregressive visual generation primarily follows three paradigms. The first, exemplified by VQGAN [18] and its successors [18, 21, 22, 26, 30, 34, 39, 40, 49, 52, 60, 61, 64], adopts a GPT-like sequential next-token prediction approach. The second, pioneered by MaskGIT [7] and extended by various works [2, 8, 15, 25, 31, 35, 59, 67, 69], employs a BERT-like masked autoregressive process. The third, introduced by VAR [57] and further developed in subsequent research [17, 28, 36, 42, 47, 53, 68, 74], generates images through a progressive next-scale refinement process. Our work builds upon the MaskGIT paradigm, extending it into a hybrid generation framework for efficient text-to-image synthesis.

3. Method

In this section, we first introduce Deep Compression Hybrid Tokenizer (DC-HT), a 2D tokenizer for autoregressive generation that achieves a spatial compression ratio of $32\times$ and our three-stage adaptation training strategy to guarantee its

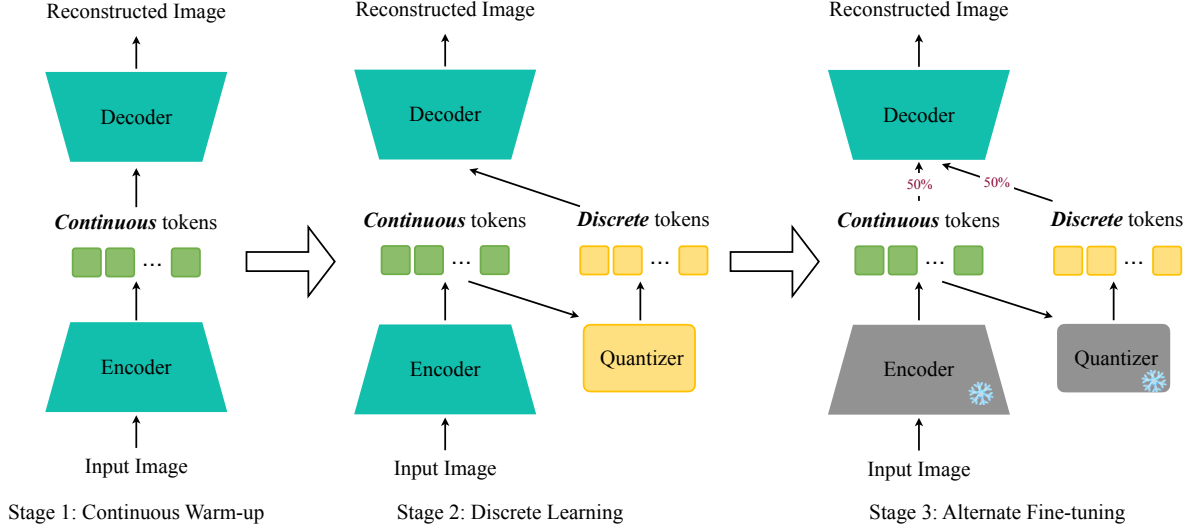


Figure 3. Illustration of Our Three-Stage Adaptation Training Strategy for DC-HT.

decent reconstruction performance. Next, we present DC-AR, an efficient masked autoregressive text-to-image generation framework built upon DC-HT.

3.1. Deep Compression Hybrid Tokenizer

While existing 1D tokenizers used in autoregressive modeling can achieve high compression ratios, they discard the 2D spatial correspondence between pixel patches, limiting their generalizability across different resolutions. To address this, we adopt the 2D discrete tokenizer framework, which includes a CNN-based encoder Enc , a CNN-based decoder Dec , and a vector-quantized (VQ) quantizer $Quant$. We adopt the same model architecture [5] as DC-AE [11], as it delivers state-of-the-art reconstruction quality in continuous tokenization with high compression ratios. Additionally, we find that discrete tokenization is highly sensitive during the codebook training process. Under a high spatial compression ratio, we observe directly training the 2D discrete deep compression tokenizer results in poor reconstruction quality (Table 4). In this work, we propose to enhance it with hybrid tokenization and a three-stage adaptation strategy to mitigate quality loss.

Hybrid Tokenization. Given an input image \mathbf{I} , the reconstruction process can proceed via either a *discrete path* or a *continuous path*. In the *discrete path*, the input image \mathbf{I} is first compressed by the CNN encoder Enc into a latent representation of continuous tokens $\mathbf{Z} = Enc(\mathbf{I})$, followed by the VQ process $\mathbf{Z}_q = Quant(\mathbf{Z})$ to obtain discrete tokens. The discrete tokens \mathbf{Z}_q are then passed through the CNN decoder Dec to reconstruct the image $\hat{\mathbf{I}} = Dec(\mathbf{Z}_q)$. The reconstruction loss and GAN loss between \mathbf{I} and $\hat{\mathbf{I}}$ are computed to train the tokenizer. In the *continuous path*,

the quantization step is skipped, and the continuous latent \mathbf{Z} is directly fed into the decoder Dec to obtain the reconstructed image $\hat{\mathbf{I}} = Dec(\mathbf{Z})$. According to HART, a critical property of the hybrid tokenizer for successful generation is its ability to decode both continuous tokens \mathbf{Z} and discrete tokens \mathbf{Z}_q effectively. It ensures that the two types of tokens remain sufficiently similar from the decoder’s perspective, facilitating easier modeling of their residual tokens, defined as $\mathbf{Z}_r = \mathbf{Z} - \mathbf{Z}_q$, during the generation process.

Three-stage Adaptation Training Strategy. Hybrid tokenization alone cannot fully resolve the reconstruction quality drop, as it faces the inherent conflict between discrete and continuous latent spaces. We find directly applying the alternate training strategy from HART [53] leads to unsatisfactory reconstruction results. We propose a Three-Stage Adaptation Training Strategy to tackle this challenge. The detailed training pipeline is illustrated in Figure 3.

The first stage, denoted as *continuous warm-up*, focuses solely on the *continuous path*. This stage is relatively short and aims to initialize the encoder with weights suitable for the reconstruction task. The second stage, denoted as *discrete learning*, activates only the *discrete path*. Here, the goal is to train the tokenizer to learn a stable latent space and enable it to reconstruct images effectively. The final stage, *alternate fine-tuning*, randomly selects either the *continuous path* or the *discrete path* for each image with equal probability (50%) to fine-tune the tokenizer. During this stage, the encoder and quantizer are frozen, and only the decoder is fine-tuned. This stage ensures that the decoder can effectively handle both continuous and discrete tokens.

By breaking down the training process into these three stages, our strategy effectively addresses the abovementioned issues, improving the rFID from 1.92 to 1.60 and

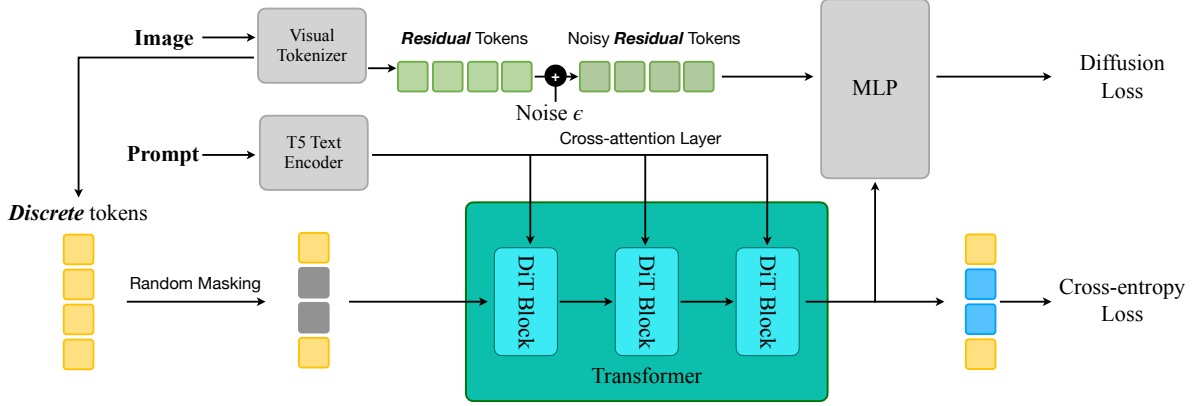


Figure 4. **Training Workflow of DC-AR.** Our visual tokenizer first decomposes the input image into discrete and residual continuous tokens. As a hybrid generation framework, we design DC-AR to model both types of tokens effectively. We use a cross-entropy loss through the mask-prediction objective to learn discrete tokens. Simultaneously, the hidden states generated by the transformer serve as conditions for an MLP, which predicts the residual tokens using a diffusion loss. The input prompt is injected into the transformer via cross-attention layers to incorporate textual guidance.

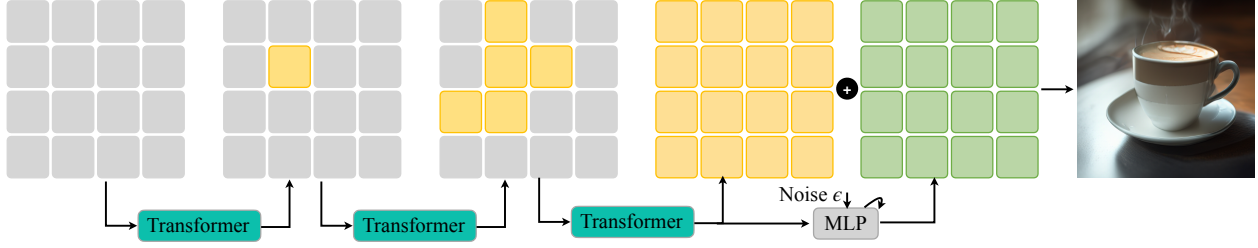


Figure 5. **Inference Workflow of DC-AR.** The process begins with a fully masked state, where we progressively predict discrete tokens using an unmasking schedule. Once we generate all discrete tokens, the final hidden states from the transformer are utilized as conditions for the diffusion head, which predicts the residual tokens through a denoising schedule. The discrete and residual tokens are combined through summation and decoded to produce the final output image. This two-stage approach ensures structural coherence and fine-grained detail in the generated image.

discrete-rFID (rFID for the discrete path) from 6.18 to 5.13.

3.2. Hybrid Masked Autoregressive Model

To fully harness the capabilities of DC-HT, we build DC-AR, a masked autoregressive framework designed to generate high-resolution images under textual guidance efficiently. Figure 4 illustrates our general framework. A text model extracts textual embeddings from input prompts, which are then integrated into transformer blocks via cross-attention to provide textual guidance. During training, we mask a random subset of discrete tokens and train the transformer model to predict these masked tokens using a cross-entropy loss. Simultaneously, the hidden states produced by the transformer model serve as conditional inputs for predicting the residual tokens through a lightweight diffusion MLP head, optimized using a diffusion loss [35].

Figure 5 demonstrates our inference pipeline. All discrete tokens are predicted iteratively through a progressive unmasking schedule, starting from a fully masked state.

Once we generate all discrete tokens, the final hidden states from the transformer are utilized as conditions for the diffusion head, which predicts the residual tokens through a denoising schedule. We then sum the predicted discrete and residual tokens to obtain the final continuous tokens, which we use to produce the generated image with our decoder.

A key design choice in our hybrid generation framework is that *only discrete tokens* are involved in the forward process of our transformer model. This approach is grounded in the principle that residual tokens should exclusively serve a refining function without altering the overall structure of the generated images. This design is critical, as empirical evidence [7] has shown that discrete token-based MaskGIT typically requires as few as eight steps to achieve near-optimal generation performance. In contrast, continuous token-based MAR [35] needs 64 steps to reach optimal performance (please refer to Appendix A.5), leading to significantly higher inference costs. By relying on discrete tokens for the transformer prediction process and residual

Tokenizer	Type	Resolution Generalizable?	# Tokens	rFID↓	PSNR↑	SSIM↑	LPIPS↓
ImageNet 256×256							
TiTok [71]	1D-Discrete	✗	64	1.70	17.06	0.4021	0.3840
TA-TiTok (VQ) [31]	1D-Discrete	✗	64	2.68	–	–	–
TA-TiTok (KL) [31]	1D-Continuous	✗	64	1.47	–	–	–
TexTok* [73]	1D-Continuous	✗	64	1.53	20.10	0.5618	0.2126
DC-HT (Ours)	2D-Hybrid	✓	64	1.60	21.50	0.5676	0.2221
ImageNet 512×512							
TiTok [71]	1D-Discrete	✗	128	1.37	–	–	–
TexTok* [73]	1D-Continuous	✗	128	0.97	22.27	0.6230	0.2365
TexTok* [73]	1D-Continuous	✗	256	0.73	24.45	0.6682	0.1875
DC-HT (Ours)	2D-Hybrid	✓	256	0.83	23.53	0.6315	0.2236

Table 1. **Image Reconstruction Results on ImageNet.** * indicates that the results of TexTok were computed on 50K samples from the ImageNet training set instead of the ImageNet validation set. DC-HT consistently demonstrates competitive performance compared to other 1D tokenizers across all benchmarks at the same compression ratio while maintaining generalizability across different resolutions.

tokens for refinement, we ensure that our framework maintains the high sampling efficiency of discrete token-based approaches like MaskGIT while achieving superior image generation quality.

As discussed in Sec. 3.1, a key advantage of our 2D spatial tokenizer design over 1D tokenizers is its ability to generalize seamlessly across different resolutions, producing tokens that reside in the same latent space. Leveraging this property, we adopt a two-stage training strategy to train an image generation model for 512×512 images efficiently. First, using a relatively long training schedule, we pre-train our model on 256×256 images. Subsequently, we fine-tune the pre-trained 256×256 model on 512×512 images to obtain the final model, which converges rapidly due to the shared latent space. As demonstrated in Sec. 4.3, this training pipeline reduces GPU hours by at least 1.9× compared to training the 512×512 model from scratch, significantly enhancing training efficiency.

4. Experiments

4.1. Setups

Models. For the tokenizer, we adopt the DC-AE-f32c32 architecture from Chen et al. [11], featuring a spatial compression ratio of 32× and a latent channel size of 32. We configure the codebook to $N = 16384$. For the generator, we utilize the PixArt- α [14] architecture for our transformer model, with its adaptive norm layers removed. It consists of 28 layers and a width of 1152, amounting to 634M parameters. The diffusion head comprises 6 MLP layers, totaling 37M parameters. To ensure computational efficiency and accessibility for research environments, we employ T5-base [48] as our text encoder, which contains 109M parameters.

Evaluation and Datasets. For the tokenizer, we use the training split of ImageNet [19] as our training dataset, resizing each image to 256×256. To assess the reconstruction performance of the tokenizer, we evaluate reconstruction FID [29] (rFID), peak signal-to-noise ratio (PSNR), structural similarity index measure (SSIM), and learned perceptual image patch similarity (LPIPS) [75] on the ImageNet validation set at resolutions of 256×256 and 512×512. For the text-to-image generator, we employ JourneyDB [51] and an internal MidJourney-style synthetic dataset, where each data point consists of an image-caption pair, where the captions are generated using VILA1.5-13B [37]. To evaluate generation performance, we report generation FID (gFID) on MJHQ-30K [33] to measure aesthetic quality and the GenEval [27] score to quantify the alignment between input prompts and generated images.

Efficiency Profiling. We profile the latency and throughput on an NVIDIA A100 GPU. We measure the throughput with a batch size of 16 and the latency with a batch size of 1. We use float16 precision for all cases.

4.2. Main Results

Image Tokenization. The quantitative results presented in Tab. 1 demonstrate that DC-HT achieves reconstruction performance on par with 1D compact tokenizers while maintaining high compression ratios. Notably, DC-HT is trained exclusively on 256×256 images yet delivers competitive performance at 512×512 resolution, whereas models for 1D tokenizers require separate training on both 256×256 and 512×512 images. This advantage stems from DC-HT’s retention of the resolution generalizability inherent to 2D tokenizers, a capability that 1D tokenizers lack.

Method	Type	#Params	Resolution	#Steps	gFID↓	Latency (s)	Throughput (images/s)
SDXL [46]	Diffusion	2.6B	1024 × 1024	20	6.63	1.4*	2.1*
PixArt- α [14]	Diffusion	630M	512 × 512	20	6.14	1.2	1.7
PixArt- Σ [12]	Diffusion	630M	512 × 512	20	6.34	1.2	1.7
SD3-medium [24]	Diffusion	2B	1024 × 1024	28	11.92	–	–
Playground v2.5 [33]	Diffusion	2B	1024 × 1024	20	6.09	–	–
Sana-0.6B [65]	Diffusion	590M	512 × 512	20	5.67	0.8	6.7
Show-o [67]	Mask. AR	1.3B	512 × 512	12	14.59	1.1	1.3
TA-TiTok (VQ) [31]	Mask. AR	568M	256 × 256	16	7.74	–	–
TA-TiTok (KL) [31]	Mask. AR	602M	256 × 256	32	7.24	–	–
DC-AR (Ours)	Mask. AR	671M	512 × 512	12	5.49	0.4	10.3

Table 2. **Text-to-Image Generation Results on MJHQ-30K.** We evaluate DC-AR against state-of-the-art diffusion and masked autoregressive models. * denotes that we report the latency and throughput for generating 512×512 images. The results demonstrate that DC-AR achieves comparable image generation quality while offering significant efficiency gains: **2.0-3.5**× lower latency and **1.5-7.9**× higher throughput compared to existing methods when generating 512×512 images.

Method	Type	#Params	S. Obj	T. Obj	Count	Colors	Position	C. Attri.	Overall
SDXL [46]	Diffusion	2.6B	0.98	0.74	0.39	0.85	0.15	0.23	0.55
PixArt- α [14]	Diffusion	630M	0.96	0.49	0.47	0.79	0.06	0.11	0.48
PixArt- Σ [12]	Diffusion	630M	0.98	0.59	0.50	0.80	0.10	0.15	0.52
SD3-medium [24]	Diffusion	2B	0.98	0.74	0.63	0.67	0.34	0.36	0.62
Playground v2.5 [33]	Diffusion	2B	0.98	0.77	0.52	0.84	0.11	0.17	0.56
Sana-0.6B [65]	Diffusion	590M	0.99	0.76	0.64	0.88	0.18	0.39	0.64
Show-o [67]	Mask. AR	1.3B	0.98	0.80	0.66	0.84	0.31	0.50	0.68
TA-TiTok (VQ) [31]	Mask. AR	568M	0.98	0.57	0.46	0.80	0.11	0.25	0.53
TA-TiTok (KL) [31]	Mask. AR	602M	0.99	0.57	0.36	0.80	0.11	0.29	0.52
Fluid [25]	Mask. AR	665M	0.96	0.73	0.51	0.77	0.42	0.51	0.65
Meisronic [2]	Mask. AR	1.0B	0.99	0.66	0.42	0.86	0.10	0.22	0.54
DC-AR (Ours)	Mask. AR	671M	1.00	0.75	0.52	0.90	0.45	0.51	0.69

Table 3. **Text-to-Image Generation Results on GenEval.** The results demonstrate that DC-AR achieves state-of-the-art performance compared to other methods of similar scale.

Text-to-Image Generation. We present quantitative text-to-image generation results in Tab. 2 and Tab. 3. On the MJHQ-30K benchmark, DC-AR achieves the state-of-the-art gFID score of 5.49 compared to leading diffusion models and other masked autoregressive models. Notably, DC-AR accomplishes this with significantly lower inference costs, requiring only 12 steps. For 512×512 image generation, DC-AR demonstrates 2.0× and 3.5× lower latency than Sana-0.6B and SD-XL, respectively, alongside 1.5× and 7.9× higher throughput than Sana-0.6B and Show-o, respectively. On the GenEval benchmark, DC-AR achieves an overall score of 0.69, matching the state-of-the-art masked autoregressive model Show-o (within 0.01) while being 2× smaller in scale. Furthermore, DC-AR outperforms other models of similar scale by at least 0.04. Additionally, we provide qualitative samples comparing the generation re-

sults of DC-AR with other advanced models in Fig. 2. The quantitative and qualitative results underscore DC-AR’s capabilities as a cutting-edge text-to-image generation framework with superior efficiency.

4.3. Ablation Studies and Analysis

We evaluate the key design choices in DC-AR by examining the following aspects: the effectiveness of our hybrid design over discrete-only baseline, the advantage of our three-stage adaptation strategy for tokenizer training, the training efficiency gains enabled by our resolution generalizable tokenizer for the generator, and the efficiency advantages of our hybrid generation framework in terms of sampling steps.

Effectiveness of the hybrid design. Compared to traditional autoregressive methods that rely solely on discrete tokens, the hybrid tokenization and generation design en-

	rFID ↓	gFID ↓	GenEval ↑	Throughput (images/s)
DC-AR	1.60	5.50	0.69	10.3
Discrete-only	5.13	6.71	0.66	11.4

Table 4. The hybrid design allows DC-AR to surpass the discrete-only baseline across all evaluation metrics, while incurring only 10% additional overhead.

	Discrete-rFID ↓	rFID ↓
Discrete Training + Alternate Fine-tuning	5.93	1.76
Continuous Warm-up + Alternate Training	6.18	1.92
Three-Stage Adaptation	5.13	1.60

Table 5. The Three-Stage Adaptation Strategy outperforms alternate training strategies for our hybrid tokenizer.

hances the representation capability of DC-AR, resulting in improved performance. To validate this, we compare DC-AR with a discrete-only baseline that excludes the continuous path, residual tokens, and the diffusion head from DC-AR. We present the results in Tab. 4. DC-AR outperforms the discrete-only baseline across various comprehensive metrics while incurring only 10% additional overhead, demonstrating our hybrid formulation’s effectiveness. Additionally, qualitative examples demonstrating how the hybrid design enhances generation quality by capturing finer details are provided in Fig. 9 of Appendix A.5.

Three-stage Adaptation Training Strategy. We evaluate our three-stage adaptation strategy for training the hybrid tokenizer with a compression ratio $32\times$ against two alternative methods, as shown in Tab. 5. The first alternative strategy omits the continuous warm-up stage, which leads to increased difficulty in learning the discrete latent space, resulting in poorer discrete-rFID and continuous-rFID performance for the final tokenizer. The second alternative strategy proceeds directly to the alternate training stage after the continuous warm-up, resembling the alternate fine-tuning stage but with all components trainable. This approach degrades both discrete-rFID and continuous-rFID due to the conflict between the discrete and continuous latent space because the latent space is trainable. Our three-stage strategy effectively addresses these issues, ensuring balanced and optimized performance.

Training Efficiency Benefit. As discussed in 3.2, our resolution-generalizable tokenizer enables an effective “pre-training then fine-tuning” strategy for the 512×512 model. This approach begins with pre-training at 256×256 resolution, followed by fine-tuning at the target 512×512 resolution. In contrast, models with single-resolution tokenizers can only be trained at the target resolution from scratch. Tab. 6 quantitatively shows that our strategy reduces training costs by more than $1.9\times$ when compared to

	Training Steps	GPU Hours	gFID ↓
Pre-training + Finetuning	200K (256) + 50K (512)	760	5.50
Training from scratch	200K (512)	1440	6.64

Table 6. Our “pre-training then fine-tuning” strategy reduces the training cost by more than $1.9\times$ for training a 512×512 model.

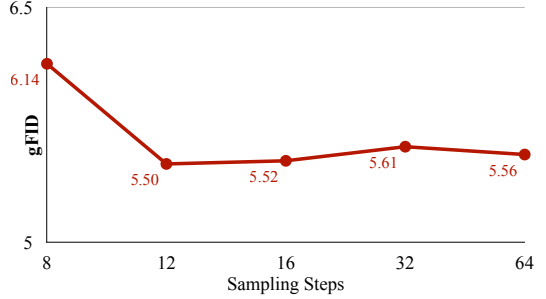


Figure 6. **Results of gFID under Different Sampling Steps.** Our hybrid generation pipeline, dominated by discrete tokens, allows DC-AR to achieve exceptional quality with just 12 sampling steps. In contrast to MAR-based methods, which require numerous steps to attain optimal performance, this reduced sampling demand grants DC-AR significant efficiency advantages.

training from scratch while maintaining superior generation quality, as measured by gFID scores.

Inference Efficiency Benefit. Fig. 6 demonstrates the gFID results of DC-AR under different sampling steps. Our discrete token dominated generation pipeline enables DC-AR to achieve optimal image quality with 12 sampling steps. In contrast, MAR-based [35] models require numerous steps to reach optimal performance. This reduced demand in sampling steps brings DC-AR great efficiency advantages without compromising generation quality.

5. Conclusion

This paper presents DC-AR, a novel and efficient masked autoregressive text-to-image generation framework. While modern diffusion models can leverage tokenizers with high compression ratios, autoregressive models encounter significant challenges when adopting the same approach. To address this, we introduce DC-HT, a 2D hybrid tokenizer that achieves a $32\times$ spatial compression ratio while maintaining exceptional reconstruction fidelity. Building on DC-HT, DC-AR is a masked autoregressive generation framework capable of effectively generating discrete and residual tokens to synthesize images. By first predicting structural elements through discrete tokens and then refining details using residual tokens, DC-AR generates high-quality images in just 12 steps. This approach delivers $1.5\text{-}7.9\times$ higher throughput and $2.0\text{-}3.5\times$ lower latency compared to state-of-the-art diffusion and masked autoregressive models.

References

- [1] Roman Bachmann, Jesse Allardice, David Mizrahi, Enrico Fini, Oğuzhan Fatih Kar, Elmira Amirloo, Alaaeldin El-Nouby, Amir Zamir, and Afshin Dehghan. Flextok: Resampling images into 1d token sequences of flexible length. *arXiv preprint arXiv:2502.13967*, 2025. 3
- [2] Jinbin Bai, Tian Ye, Wei Chow, Enxin Song, Qing-Guo Chen, Xiangtai Li, Zhen Dong, Lei Zhu, and Shuicheng Yan. Meissonic: Revitalizing masked generative transformers for efficient high-resolution text-to-image synthesis. *arXiv preprint arXiv:2410.08261*, 2024. 2, 3, 7
- [3] Fan Bao, Shen Nie, Kaiwen Xue, Yue Cao, Chongxuan Li, Hang Su, and Jun Zhu. All are worth words: A vit backbone for diffusion models. In *Proceedings of the IEEE/CVF conference on computer vision and pattern recognition*, pages 22669–22679, 2023. 3
- [4] BlackForest Labs. Flux, 2024. 2
- [5] Han Cai, Junyan Li, Muyan Hu, Chuang Gan, and Song Han. Efficientvit: Lightweight multi-scale attention for high-resolution dense prediction. In *Proceedings of the IEEE/CVF International Conference on Computer Vision*, pages 17302–17313, 2023. 4
- [6] Han Cai, Muyang Li, Qingsheng Zhang, Ming-Yu Liu, and Song Han. Condition-aware neural network for controlled image generation. In *Proceedings of the IEEE/CVF Conference on Computer Vision and Pattern Recognition*, pages 7194–7203, 2024. 3
- [7] Huiwen Chang, Han Zhang, Lu Jiang, Ce Liu, and William T Freeman. Maskgit: Masked generative image transformer. In *Proceedings of the IEEE/CVF conference on computer vision and pattern recognition*, pages 11315–11325, 2022. 2, 3, 5
- [8] Huiwen Chang, Han Zhang, Jarred Barber, AJ Maschinot, Jose Lezama, Lu Jiang, Ming-Hsuan Yang, Kevin Murphy, William T Freeman, Michael Rubinstein, et al. Muse: Text-to-image generation via masked generative transformers. *arXiv preprint arXiv:2301.00704*, 2023. 2, 3
- [9] Hao Chen, Ze Wang, Xiang Li, Ximeng Sun, Fangyi Chen, Jiang Liu, Jindong Wang, Bhiksha Raj, Zicheng Liu, and Emad Barsoum. Softvq-vae: Efficient 1-dimensional continuous tokenizer. *arXiv preprint arXiv:2412.10958*, 2024. 3
- [10] Hao Chen, Yujin Han, Fangyi Chen, Xiang Li, Yidong Wang, Jindong Wang, Ze Wang, Zicheng Liu, Difan Zou, and Bhiksha Raj. Masked autoencoders are effective tokenizers for diffusion models. *arXiv preprint arXiv:2502.03444*, 2025. 3
- [11] Junyu Chen, Han Cai, Junsong Chen, Enze Xie, Shang Yang, Haotian Tang, Muyang Li, Yao Lu, and Song Han. Deep compression autoencoder for efficient high-resolution diffusion models. *arXiv preprint arXiv:2410.10733*, 2024. 2, 3, 4, 6
- [12] Junsong Chen, Chongjian Ge, Enze Xie, Yue Wu, Lewei Yao, Xiaozhe Ren, Zhongdao Wang, Ping Luo, Huchuan Lu, and Zhenguo Li. Pixart- σ : Weak-to-strong training of diffusion transformer for 4k text-to-image generation. In *European Conference on Computer Vision*, pages 74–91. Springer, 2024. 3, 7
- [13] Junsong Chen, Yue Wu, Simian Luo, Enze Xie, Sayak Paul, Ping Luo, Hang Zhao, and Zhenguo Li. Pixart- $\{\delta\}$: Fast and controllable image generation with latent consistency models. *arXiv preprint arXiv:2401.05252*, 2024.
- [14] Junsong Chen, Jincheng Yu, Chongjian Ge, Lewei Yao, Enze Xie, Zhongdao Wang, James T Kwok, Ping Luo, Huchuan Lu, and Zhenguo Li. Pixart- α : Fast training of diffusion transformer for photorealistic text-to-image synthesis. In *ICLR*, 2024. 3, 6, 7
- [15] Wenchao Chen, Liqiang Niu, Ziyao Lu, Fandong Meng, and Jie Zhou. Maskmamba: A hybrid mamba-transformer model for masked image generation. *arXiv preprint arXiv:2409.19937*, 2024. 2, 3
- [16] Xiaokang Chen, Zhiyu Wu, Xingchao Liu, Zizheng Pan, Wen Liu, Zhenda Xie, Xingkai Yu, and Chong Ruan. Janus-pro: Unified multimodal understanding and generation with data and model scaling. *arXiv preprint arXiv:2501.17811*, 2025. 3
- [17] Zigeng Chen, Xinyin Ma, Gongfan Fang, and Xinchao Wang. Collaborative decoding makes visual auto-regressive modeling efficient. *arXiv preprint arXiv:2411.17787*, 2024. 3
- [18] Katherine Crowson, Stella Biderman, Daniel Kornis, Dashiell Stander, Eric Hallahan, Louis Castricato, and Edward Raff. Vqgan-clip: Open domain image generation and editing with natural language guidance. In *European conference on computer vision*, pages 88–105. Springer, 2022. 3
- [19] Jia Deng, Wei Dong, Richard Socher, Li-Jia Li, Kai Li, and Li Fei-Fei. Imagenet: A large-scale hierarchical image database. In *2009 IEEE conference on computer vision and pattern recognition*, pages 248–255. Ieee, 2009. 2, 6
- [20] Jacob Devlin, Ming-Wei Chang, Kenton Lee, and Kristina Toutanova. Bert: Pre-training of deep bidirectional transformers for language understanding. In *Proceedings of the 2019 conference of the North American chapter of the association for computational linguistics: human language technologies, volume 1 (long and short papers)*, pages 4171–4186, 2019. 2
- [21] Ming Ding, Zhuoyi Yang, Wenyi Hong, Wendi Zheng, Chang Zhou, Da Yin, Junyang Lin, Xu Zou, Zhou Shao, Hongxia Yang, et al. Cogview: Mastering text-to-image generation via transformers. *Advances in neural information processing systems*, 34:19822–19835, 2021. 3
- [22] Ming Ding, Wendi Zheng, Wenyi Hong, and Jie Tang. Cogview2: Faster and better text-to-image generation via hierarchical transformers. *Advances in Neural Information Processing Systems*, 35:16890–16902, 2022. 3
- [23] Patrick Esser, Robin Rombach, and Bjorn Ommer. Taming transformers for high-resolution image synthesis. In *Proceedings of the IEEE/CVF conference on computer vision and pattern recognition*, pages 12873–12883, 2021. 3
- [24] Patrick Esser, Sumith Kulal, Andreas Blattmann, Rahim Entezari, Jonas Müller, Harry Saini, Yam Levi, Dominik Lorenz, Axel Sauer, Frederic Boesel, et al. Scaling rectified flow transformers for high-resolution image synthesis. In *Forty-first international conference on machine learning*, 2024. 2, 3, 7

- [25] Lijie Fan, Tianhong Li, Siyang Qin, Yuanzhen Li, Chen Sun, Michael Rubinstein, Deqing Sun, Kaiming He, and Yonglong Tian. Fluid: Scaling autoregressive text-to-image generative models with continuous tokens. *arXiv preprint arXiv:2410.13863*, 2024. 2, 3, 7
- [26] Oran Gafni, Adam Polyak, Oron Ashual, Shelly Sheynin, Devi Parikh, and Yaniv Taigman. Make-a-scene: Scene-based text-to-image generation with human priors. In *European Conference on Computer Vision*, pages 89–106. Springer, 2022. 3
- [27] Dhruva Ghosh, Hannaneh Hajishirzi, and Ludwig Schmidt. Geneval: An object-focused framework for evaluating text-to-image alignment. *Advances in Neural Information Processing Systems*, 36:52132–52152, 2023. 6
- [28] Jian Han, Jinlai Liu, Yi Jiang, Bin Yan, Yuqi Zhang, Zehuan Yuan, Bingyue Peng, and Xiaobing Liu. Infinity: Scaling bit-wise autoregressive modeling for high-resolution image synthesis. *arXiv preprint arXiv:2412.04431*, 2024. 2, 3
- [29] Martin Heusel, Hubert Ramsauer, Thomas Unterthiner, Bernhard Nessler, and Sepp Hochreiter. Gans trained by a two time-scale update rule converge to a local nash equilibrium. *Advances in neural information processing systems*, 30, 2017. 6
- [30] Doohyuk Jang, Sihwan Park, June Yong Yang, Yeonsung Jung, Jihun Yun, Souvik Kundu, Sung-Yub Kim, and Eunho Yang. Lantern: Accelerating visual autoregressive models with relaxed speculative decoding. *arXiv preprint arXiv:2410.03355*, 2024. 2, 3
- [31] Dongwon Kim, Ju He, Qihang Yu, Chenglin Yang, Xiaohui Shen, Suha Kwak, and Liang-Chieh Chen. Democratizing text-to-image masked generative models with compact text-aware one-dimensional tokens. *arXiv preprint arXiv:2501.07730*, 2025. 2, 3, 6, 7, 5
- [32] Dan Kondratyuk, Lijun Yu, Xiuye Gu, José Lezama, Jonathan Huang, Grant Schindler, Rachel Hornung, Vignesh Birodkar, Jimmy Yan, Ming-Chang Chiu, et al. Videopoet: A large language model for zero-shot video generation. In *ICML*, 2024. 2
- [33] Daiqing Li, Aleks Kamko, Ehsan Akhgari, Ali Sabet, Linmiao Xu, and Suhail Doshi. Playground v2. 5: Three insights towards enhancing aesthetic quality in text-to-image generation. *arXiv preprint arXiv:2402.17245*, 2024. 3, 6, 7
- [34] Tianhong Li, Huiwen Chang, Shlok Mishra, Han Zhang, Dina Katabi, and Dilip Krishnan. Mage: Masked generative encoder to unify representation learning and image synthesis. In *Proceedings of the IEEE/CVF Conference on Computer Vision and Pattern Recognition*, pages 2142–2152, 2023. 2, 3
- [35] Tianhong Li, Yonglong Tian, He Li, Mingyang Deng, and Kaiming He. Autoregressive image generation without vector quantization. *Advances in Neural Information Processing Systems*, 37:56424–56445, 2025. 3, 5, 8
- [36] Xiang Li, Kai Qiu, Hao Chen, Jason Kuen, Zhe Lin, Rita Singh, and Bhiksha Raj. Controlvar: Exploring controllable visual autoregressive modeling. *arXiv preprint arXiv:2406.09750*, 2024. 3
- [37] Ji Lin, Hongxu Yin, Wei Ping, Pavlo Molchanov, Mohammad Shoybi, and Song Han. Vila: On pre-training for visual language models. In *Proceedings of the IEEE/CVF conference on computer vision and pattern recognition*, pages 26689–26699, 2024. 6
- [38] Bingchen Liu, Ehsan Akhgari, Alexander Visheratin, Aleks Kamko, Linmiao Xu, Shivam Shrirao, Chase Lambert, Joao Souza, Suhail Doshi, and Daiqing Li. Playground v3: Improving text-to-image alignment with deep-fusion large language models. *arXiv preprint arXiv:2409.10695*, 2024. 2, 3
- [39] Dongyang Liu, Shitian Zhao, Le Zhuo, Weifeng Lin, Yu Qiao, Hongsheng Li, and Peng Gao. Lumina-mgpt: Illuminate flexible photorealistic text-to-image generation with multimodal generative pretraining. *arXiv preprint arXiv:2408.02657*, 2024. 3
- [40] Hao Liu, Wilson Yan, Matei Zaharia, and Pieter Abbeel. World model on million-length video and language with blockwise ringattention. *arXiv preprint arXiv:2402.08268*, 2024. 3
- [41] Bingqi Ma, Zhuofan Zong, Guanglu Song, Hongsheng Li, and Yu Liu. Exploring the role of large language models in prompt encoding for diffusion models. In *The Thirty-eighth Annual Conference on Neural Information Processing Systems*, 2024. 3
- [42] Xiaoxiao Ma, Mohan Zhou, Tao Liang, Yalong Bai, Tiejun Zhao, Huaian Chen, and Yi Jin. Star: Scale-wise text-to-image generation via auto-regressive representations. *arXiv preprint arXiv:2406.10797*, 2024. 3
- [43] OpenAI. Hello gpt-4o, 2024. 2
- [44] William Peebles and Saining Xie. Scalable diffusion models with transformers. In *Proceedings of the IEEE/CVF international conference on computer vision*, pages 4195–4205, 2023. 3
- [45] Pablo Pernias, Dominic Rampas, Mats Leon Richter, Christopher Pal, and Marc Aubreville. Würstchen: An efficient architecture for large-scale text-to-image diffusion models. In *The Twelfth International Conference on Learning Representations*, 2024. 2
- [46] Dustin Podell, Zion English, Kyle Lacey, Andreas Blattmann, Tim Dockhorn, Jonas Müller, Joe Penna, and Robin Rombach. Sdxl: Improving latent diffusion models for high-resolution image synthesis. In *The Twelfth International Conference on Learning Representations*, 2023. 3, 7
- [47] Liao Qu, Huichao Zhang, Yiheng Liu, Xu Wang, Yi Jiang, Yiming Gao, Hu Ye, Daniel K Du, Zehuan Yuan, and Xinglong Wu. Tokenflow: Unified image tokenizer for multimodal understanding and generation. *arXiv preprint arXiv:2412.03069*, 2024. 3
- [48] Colin Raffel, Noam Shazeer, Adam Roberts, Katherine Lee, Sharan Narang, Michael Matena, Yanqi Zhou, Wei Li, and Peter J Liu. Exploring the limits of transfer learning with a unified text-to-text transformer. *Journal of machine learning research*, 21(140):1–67, 2020. 6
- [49] Aditya Ramesh, Mikhail Pavlov, Gabriel Goh, Scott Gray, Chelsea Voss, Alec Radford, Mark Chen, and Ilya Sutskever. Zero-shot text-to-image generation. In *International conference on machine learning*, pages 8821–8831. Pmlr, 2021. 3

- [50] Robin Rombach, Andreas Blattmann, Dominik Lorenz, Patrick Esser, and Björn Ommer. High-resolution image synthesis with latent diffusion models. In *Proceedings of the IEEE/CVF conference on computer vision and pattern recognition*, pages 10684–10695, 2022. 3
- [51] Keqiang Sun, Juntong Pan, Yuying Ge, Hao Li, Haodong Duan, Xiaoshi Wu, Renrui Zhang, Aojun Zhou, Zipeng Qin, Yi Wang, et al. Journeydb: A benchmark for generative image understanding. *Advances in neural information processing systems*, 36:49659–49678, 2023. 6
- [52] Peize Sun, Yi Jiang, Shoufa Chen, Shilong Zhang, Bingyue Peng, Ping Luo, and Zehuan Yuan. Autoregressive model beats diffusion: Llama for scalable image generation. *arXiv preprint arXiv:2406.06525*, 2024. 3
- [53] Haotian Tang, Yecheng Wu, Shang Yang, Enze Xie, Junsong Chen, Junyu Chen, Zhuoyang Zhang, Han Cai, Yao Lu, and Song Han. Hart: Efficient visual generation with hybrid autoregressive transformer. *arXiv preprint arXiv:2410.10812*, 2024. 2, 3, 4, 5
- [54] Auraflow Team. Introducing auraflow v0. 1, an open exploration of large rectified flow models, 2024. URL <https://blog.fal.ai/auraflow>, 4, 2024. 3
- [55] Gemini Team, Rohan Anil, Sebastian Borgeaud, Jean-Baptiste Alayrac, Jiahui Yu, Radu Soricut, Johan Schalkwyk, Andrew M Dai, Anja Hauth, Katie Millican, et al. Gemini: a family of highly capable multimodal models. *arXiv preprint arXiv:2312.11805*, 2023. 2
- [56] K Team. Kolos: Effective training of diffusion model for photorealistic text-to-image synthesis. *arXiv preprint*, 2024. 3
- [57] Keyu Tian, Yi Jiang, Zehuan Yuan, Bingyue Peng, and Liwei Wang. Visual autoregressive modeling: Scalable image generation via next-scale prediction. *Advances in neural information processing systems*, 37:84839–84865, 2025. 3
- [58] Aaron Van Den Oord, Oriol Vinyals, et al. Neural discrete representation learning. *Advances in neural information processing systems*, 30, 2017. 3
- [59] Ruben Villegas, Mohammad Babaeizadeh, Pieter-Jan Kin-dermans, Hernan Moraldo, Han Zhang, Mohammad Taghi Saffar, Santiago Castro, Julius Kunze, and Dumitru Erhan. Phenaki: Variable length video generation from open domain textual description. *arXiv preprint arXiv:2210.02399*, 2022. 2, 3
- [60] Xinlong Wang, Xiaosong Zhang, Zhengxiong Luo, Quan Sun, Yufeng Cui, Jinsheng Wang, Fan Zhang, Yuezhe Wang, Zhen Li, Qiyang Yu, et al. Emu3: Next-token prediction is all you need. *arXiv preprint arXiv:2409.18869*, 2024. 2, 3
- [61] Yuqing Wang, Shuhuai Ren, Zhijie Lin, Yujin Han, Haoyuan Guo, Zhenheng Yang, Difan Zou, Jiashi Feng, and Xihui Liu. Parallelized autoregressive visual generation. *arXiv preprint arXiv:2412.15119*, 2024. 3
- [62] Mark Weber, Lijun Yu, Qihang Yu, Xueqing Deng, Xiaohui Shen, Daniel Cremers, and Liang-Chieh Chen. Maskbit: Embedding-free image generation via bit tokens. *Transactions on Machine Learning Research*, 2024. 2
- [63] Chengyue Wu, Xiaokang Chen, Zhiyu Wu, Yiyang Ma, Xingchao Liu, Zizheng Pan, Wen Liu, Zhenda Xie, Xingkai Yu, Chong Ruan, et al. Janus: Decoupling visual encoding for unified multimodal understanding and generation. *arXiv preprint arXiv:2410.13848*, 2024. 2
- [64] Yecheng Wu, Zhuoyang Zhang, Junyu Chen, Haotian Tang, Dacheng Li, Yunhao Fang, Ligeng Zhu, Enze Xie, Hongxu Yin, Li Yi, et al. Vila-u: a unified foundation model integrating visual understanding and generation. *arXiv preprint arXiv:2409.04429*, 2024. 2, 3
- [65] Enze Xie, Junsong Chen, Junyu Chen, Han Cai, Haotian Tang, Yujun Lin, Zhekai Zhang, Muyang Li, Ligeng Zhu, Yao Lu, et al. Sana: Efficient high-resolution image synthesis with linear diffusion transformers. *arXiv preprint arXiv:2410.10629*, 2024. 2, 3, 7
- [66] Enze Xie, Junsong Chen, Yuyang Zhao, Jincheng Yu, Ligeng Zhu, Yujun Lin, Zhekai Zhang, Muyang Li, Junyu Chen, Han Cai, et al. Sana 1.5: Efficient scaling of training-time and inference-time compute in linear diffusion transformer. *arXiv preprint arXiv:2501.18427*, 2025. 3
- [67] Jinheng Xie, Weijia Mao, Zechen Bai, David Junhao Zhang, Weihao Wang, Kevin Qinghong Lin, Yuchao Gu, Zhijie Chen, Zhenheng Yang, and Mike Zheng Shou. Show-o: One single transformer to unify multimodal understanding and generation. *arXiv preprint arXiv:2408.12528*, 2024. 2, 3, 7
- [68] Ziyu Yao, Jialin Li, Yifeng Zhou, Yong Liu, Xi Jiang, Chengjie Wang, Feng Zheng, Yuexian Zou, and Lei Li. Car: Controllable autoregressive modeling for visual generation. *arXiv preprint arXiv:2410.04671*, 2024. 3
- [69] Jiahui Yu, Yuanzhong Xu, Jing Yu Koh, Thang Luong, Gungjan Baid, Zirui Wang, Vijay Vasudevan, Alexander Ku, Yin-fei Yang, Burcu Karagol Ayan, et al. Scaling autoregressive models for content-rich text-to-image generation. *Trans. Mach. Learn. Res.*, 2022. 2, 3
- [70] Lijun Yu, Yong Cheng, Kihyuk Sohn, José Lezama, Han Zhang, Huiwen Chang, Alexander G Hauptmann, Ming-Hsuan Yang, Yuan Hao, Irfan Essa, et al. Magvit: Masked generative video transformer. In *Proceedings of the IEEE/CVF Conference on Computer Vision and Pattern Recognition*, pages 10459–10469, 2023. 2
- [71] Qihang Yu, Mark Weber, Xueqing Deng, Xiaohui Shen, Daniel Cremers, and Liang-Chieh Chen. An image is worth 32 tokens for reconstruction and generation. *Advances in Neural Information Processing Systems*, 37:128940–128966, 2025. 2, 3, 6
- [72] Wenjun Zeng, Yuchi Liu, Ryan Mullins, Ludovic Peran, Joe Fernandez, Hamza Harkous, Karthik Narasimhan, Drew Proud, Piyush Kumar, Bhaktipriya Radharapu, et al. Shield-gemma: Generative ai content moderation based on gemma. *arXiv preprint arXiv:2407.21772*, 2024. 1
- [73] Kaiwen Zha, Lijun Yu, Alireza Fathi, David A Ross, Cordelia Schmid, Dina Katabi, and Xiuye Gu. Language-guided image tokenization for generation. *arXiv preprint arXiv:2412.05796*, 2024. 3, 6
- [74] Qian Zhang, Xiangzi Dai, Ninghua Yang, Xiang An, Ziyong Feng, and Xingyu Ren. Var-clip: Text-to-image generator with visual auto-regressive modeling. *arXiv preprint arXiv:2408.01181*, 2024. 3

- [75] Richard Zhang, Phillip Isola, Alexei A Efros, Eli Shechtman, and Oliver Wang. The unreasonable effectiveness of deep features as a perceptual metric. In *Proceedings of the IEEE conference on computer vision and pattern recognition*, pages 586–595, 2018. [6](#)

DC-AR: Efficient Masked Autoregressive Image Generation with Deep Compression Hybrid Tokenizer

Supplementary Material

A. Appendix

We provide additional information and results in the appendix, as outlined below:

- Appendix A.1: Ethics Statement, discussing about how we prevent the misuse of DC-AR.
- Appendix A.2: Implementation Details, including the training hyper-parameters for tokenizer and generator, inference hyper-parameters for generator.
- Appendix A.3: Additional text-to-image generation of DC-AR and other popular methods.
- Appendix A.4: Qualitative comparison between DC-AR and the discrete-only baseline.
- Appendix A.5: Additional experiments to help clarify the advantages of DC-AR.

A.1. Ethics Statement

The misuse of generative AI for creating NSFW (not safe for work) content continues to be a critical concern within the community. To address this, we have integrated DC-AR with ShieldGemma-2B [72], a robust LLM-based safety check model. In our implementation, user prompts are first evaluated by the safety check model to detect NSFW content, including harmful, abusive, hateful, sexually explicit, or otherwise inappropriate material targeting individuals or protected groups. If a prompt is deemed safe, it is forwarded to DC-AR for image generation. If not, the prompt is rejected and replaced with a default prompt (“A red heart”). Through rigorous testing, we have demonstrated that our safety check model effectively filters out NSFW prompts under strict thresholds, ensuring that our pipeline does not produce harmful AI-generated content.

A.2. Implementation Details

Tab. 7 and Tab. 8 present the hyper-parameters used for training the tokenizer and generator, respectively. For image generation, we employ the following sampling hyper-parameters: a randomized temperature of 4.5, a CFG (Classifier-Free Guidance) scale of 4.5, a constant CFG schedule, 12 sampling steps for discrete tokens, and 20 diffusion steps for residual tokens.

Hyper-parameters	Configuration
optimizer	Adam
β_1	0.9
β_2	0.95
discriminator loss weight	0.5
perceptual loss weight	1.0
L_1 loss weight	0.0
L_2 loss weight	1.0
weight decay	0.0
learning rate	1e-4
lr schedule	constant
batch size	128
training epochs (continuous warm-up)	10
training epochs (discrete learning)	40
training epochs (alternate fine-tuning)	10

Table 7. Training hyper-parameters for our tokenizer.

Hyper-parameters	Configuration
optimizer	Adamw
β_1	0.9
β_2	0.96
condition dropout	0.1
attention dropout	0.1
cross-entropy loss weight	1.0
diffusion loss weight	1.0
weight decay	0.03
learning rate	1e-4
lr schedule	cosine
batch size (256×256)	1024
batch size (512×512)	1024
training steps (256×256)	200K
training steps (512×512)	50K

Table 8. Training hyper-parameters for our generator.



A snow globe containing a miniature winter village.



A haunted house on a hill under a full moon.



A submarine exploring an underwater cave.



A rabbit pulling a carrot from a garden, storybook illustration.



A castle on a floating island in the clouds.



A penguin wearing sunglasses on a beach.



A train traveling through snowy mountains.



A fairy tale castle with rainbow-colored towers.



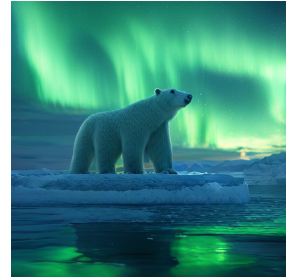
A fox wearing a scarf in the snow.



A moonlit path through a mystical forest.



A plate of cookies with a glass of milk.



A polar bear on an ice floe under the aurora borealis.



A coffee cup with steam and a heart on it.



A vintage camera on a map, travel photography style.



A squirrel holding an acorn, cartoon style.



A wooden rowboat on a misty lake at sunrise.

Figure 7. Additional text-to-image generation results of DC-AR.

A.3. Additional Text-to-image Examples

Fig. 7 and Fig. 8 includes more qualitative examples of text-to-image generation results of DC-AR.



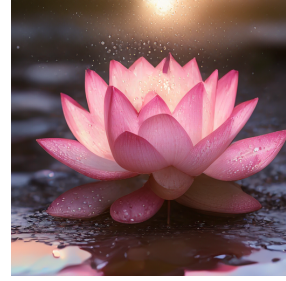
A close-up photo of a honeycomb with bees actively working, golden honey visible in cells, wings a blur of movement.



Underwater tea party with mermaids and sea turtles, coral reef in background.



Tiny house inside a terrarium, miniature garden with working lights, tilt-shift photography.



A close-up photo of a lotus flower emerging from muddy water, perfect pink petals opening toward sunlight, water droplets visible.



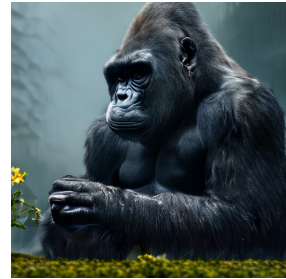
A 4k dslr image of a lemur wearing a red magician hat and a blue coat performing magic tricks with cards in a garden.



Robot barista making coffee in a steampunk café, brass pipes and gears visible.



A photo of a bonsai tree in a handcrafted ceramic pot, perfectly pruned, sitting by a window with rain droplets visible.



A silverback gorilla sitting thoughtfully in misty mountain forest, massive hands gently examining a small flower, rain-dampened fur glistening.



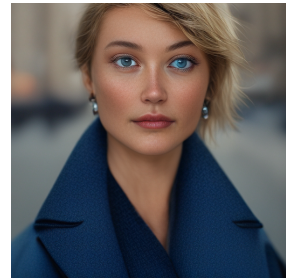
Dragon made of constellation stars flying across night sky, over mountain landscape.



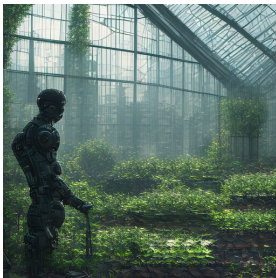
Astronaut discovering alien flowers on distant planet, sci-fi concept art, dramatic lighting.



A close-up photo of frost patterns forming intricate crystalline structures on a red maple leaf, backlit by early morning sun.



A close-up photo of a woman. She wore a blue coat. She has blue eyes and blond hair, and wears a pair of earrings. Behind are blurred city buildings and streets.



Post-apocalyptic greenhouse preserving Earth's last plant species, tended by robots, with the ruined cityscape visible through cracked glass panels.



Cosmic lighthouse keeper's cottage surrounded by aurora waves, collecting stardust in glass jars, with a telescope tracking wandering celestial bodies.



Crystalline city floating among clouds, connected by rainbow bridges, with inhabitants riding winged creatures between iridescent spires.



Witch's apothecary nestled in a hollow tree, filled with bubbling potions, sentient plants, and familiars organizing ingredients by moonlight.

Figure 8. Additional text-to-image generation results of DC-AR.

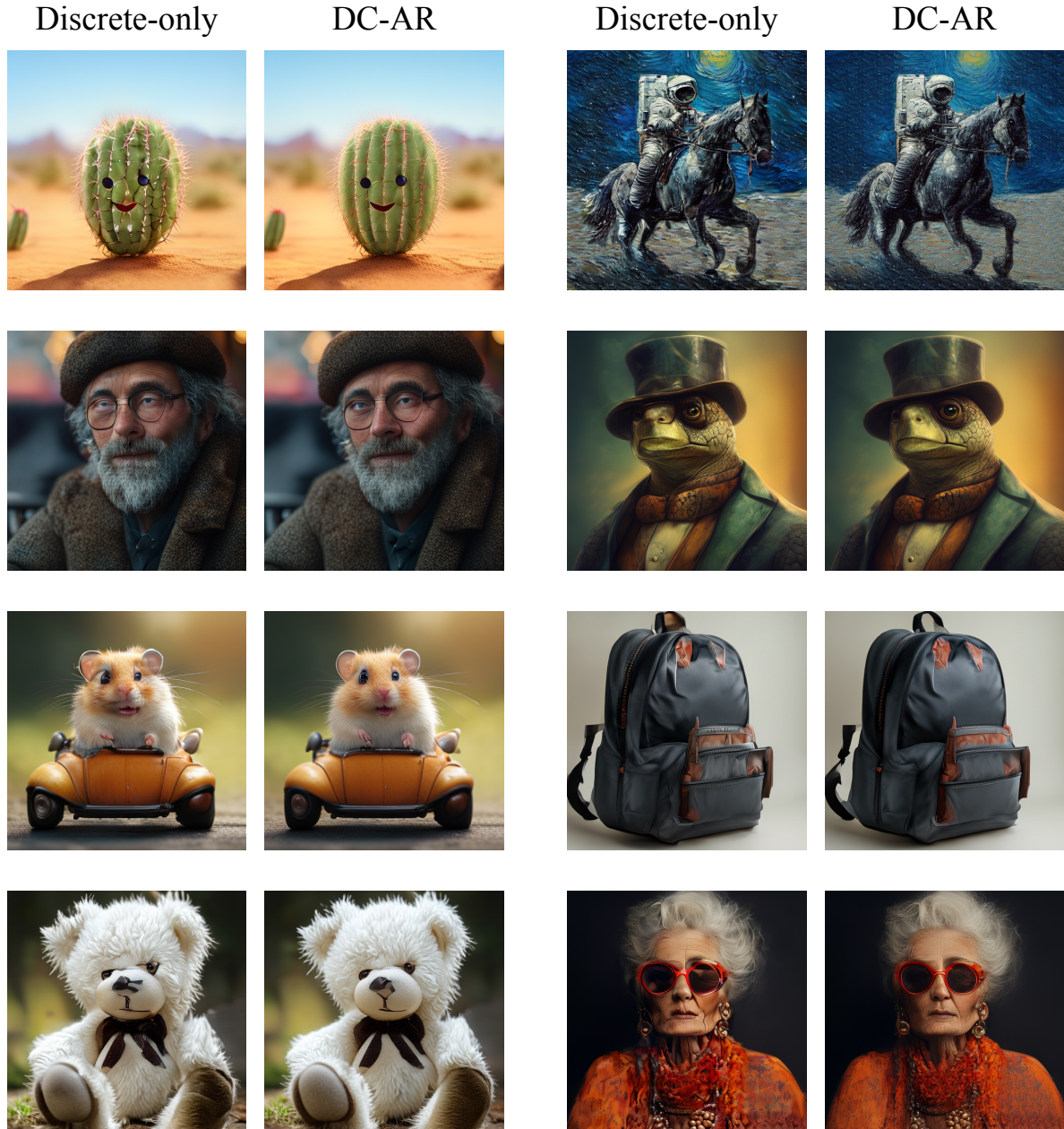


Figure 9. **Qualitative Comparison: Images Generated by DC-AR vs. the Discrete-Only Baseline.** For each pair of images, the left image is produced by the discrete-only baseline, while the right image is generated by DC-AR.

A.4. Qualitative Comparison of DC-AR and discrete-only baseline.

We present qualitative comparison examples of images generated by DC-AR and the discrete-only baseline. From these examples, it is evident that the diffusion head and residual tokens significantly enhance image refinement, particularly in capturing fine details such as eyes and textures.

A.5. Additional Experimental Results.

In this section, we provide some other experiments related to DC-AR.

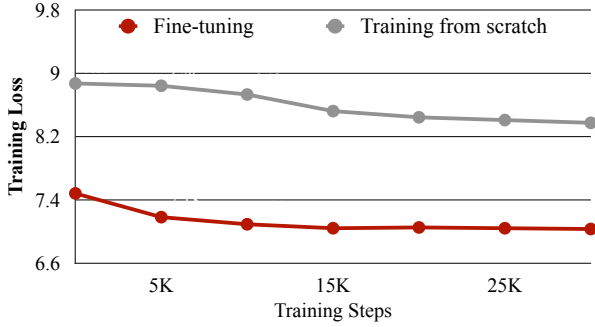


Figure 10. The resolution generalizability of DC-HT allows us to train a 512×512 model by fine-tuning from a pre-trained 256×256 model, achieving significantly faster convergence compared to training from scratch.

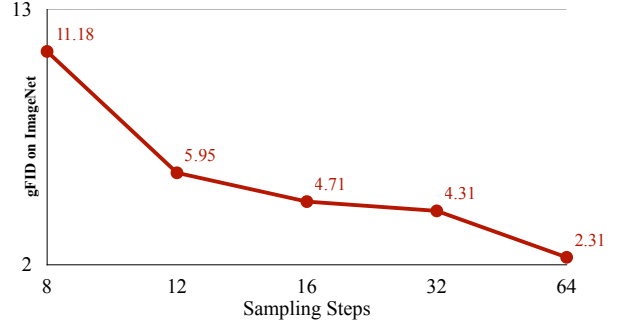


Figure 11. **gFID Results on ImageNet 256×256 for MAR-B at Different Sampling Steps.** MAR-B requires 64 sampling steps to achieve its best performance, significantly lagging behind our method, which attains optimal performance in just 12 steps.

Training Loss Curve: Fine-Tuning vs. Training from Scratch. Fig. 10 illustrates the training loss curves for fine-tuning and training from scratch on 512×512 models over the first 30K steps. It is evident that fine-tuning from a pre-trained 256×256 model enables the 512×512 model to converge significantly faster than training from scratch.

Sampling Step Requirements for MAR. Our primary motivation for adopting a hybrid generation framework, rather than following MAR’s paradigm of exclusively using continuous tokens, stems from the observation that MAR typically requires a large number of steps to achieve optimal performance. This is demonstrated in Fig. 6, where we evaluate the official MAR-B model for class-conditional image generation on ImageNet at 256×256 resolution. Despite the image token sequence length being 256, MAR-B requires 64 steps to reach its optimal performance, resulting in a substantial inference cost. In contrast, DC-AR achieves optimal performance in just 12 steps, making it significantly more efficient during sampling.

A.6. Discussion of DC-AR and Related Works.

As a novel autoregressive image generation framework, DC-AR draws inspiration from several related works in the field while introducing significant innovations that distinguish it from each of them.

Difference with MaskGen [31]. Both MaskGen and DC-AR adopt the masked autoregressive generation paradigm for text-to-image generation and employ an image tokenizer with a high compression ratio for efficient generation. However, their technical approaches to building the tokenizer and generator differ substantially. On the tokenizer side, MaskGen follows the recent trend of using a 1D compact tokenizer to achieve a high compression ratio. However, a major limitation of such 1D tokenizers is their lack of generalizability across different resolutions. Consequently, MaskGen must train separate tokenizers and generators from scratch for each resolution, leading to significantly higher training costs, especially for resolutions of 512×512 or higher. In contrast, DC-AR utilizes a single tokenizer trained on 256×256 images for all resolutions and fine-tunes the generator for higher resolutions from a pre-trained low-resolution model, resulting in much greater efficiency. On the generator side, MaskGen combines the MaskGIT paradigm for discrete token generation with the MAR paradigm for continuous token generation. In contrast, DC-AR introduces a novel hybrid generation framework that leverages the superior representation capability of continuous tokens while maintaining the high inference speed of discrete tokens.

Difference with HART [53]. HART proposes the idea of hybrid tokenization, using a transformer model to generate discrete tokens and a lightweight diffusion head to generate continuous tokens. While DC-AR inherits these ideas, it adapts them in a fundamentally different setting. HART follows the VAR paradigm, which generates images through progressive next-scale refinement. In contrast, DC-AR adopts the MaskGIT paradigm, which generates images through progressive unmasking. Although the VAR paradigm is widely recognized for its high generation quality and speed, we believe the MaskGIT paradigm offers unique advantages, including fewer tokens (VAR requires additional tokens due to its multi-scale tokenization design) and a natural suitability for image editing tasks. Building on this foundation, DC-AR introduces novel methods, such as a single-scale hybrid tokenizer with a $32 \times$ compression ratio (via our three-stage adaptation strategy) and an efficient hybrid generation framework that extends MaskGIT (via our discrete token-dominated generation pipeline). Notably, in the results section, we do not include comparisons with VAR-based methods, as we aim to focus the discussion

on how DC-AR advances the MaskGIT paradigm. In future work, we plan to explore adapting our approach to the VAR paradigm to design even more effective generation frameworks.